Eur Biophys J (2003) 32: 12–21
DOI 10.1007/s00249-002-0267-6

ARTICLE

Zuzanna Siwy · Maria E. Mycielska
Mustafa B. A. Djamgoz

Statistical and fractal analyses of rat prostate cancer cell motility in a direct current electric field: comparison of strongly and weakly metastatic cells

Received: 1 August 2002 / Revised: 17 October 2002 / Accepted: 24 October 2002 / Published online: 15 January 2003

Abstract The problems addressed here comprised (1) possible differences in galvanotactic properties of strongly versus weakly metastatic rat prostate cancer cells, with MAT-LyLu and AT-2 as examples, respectively; (2) quantitative description of the responses of the MAT-LyLu cells to direct current (dc) electric fields (EFs) of physiological strength (0.3–3 V/cm); and (3) voltage and time dependency of the cells' responses to the dcEFs. These issues were studied by application of statistical and fractal analyses of the cells' trajectories. The results showed that the MAT-LyLu cells responded strongly to the applied dcEFs by migrating towards the cathode. On the other hand, the galvanotactic response of the AT-2 cells was weak and towards the anode. Further studies of the MAT-LyLu cell motility in dcEFs of increasing strength showed that their response consisted of two voltage domains. Weaker fields (~0.6 V/cm) induced "straightening" of the cells' trajectories without the cells showing a clear tendency to move along the applied field. Stronger fields (> 0.6 V/cm) made the cells' movement oriented with respect to the direction of the applied field, without further changing the trajectories' structure. The results also showed that the cells do not perform a directed movement instantaneously after switching on a dcEF of 3 V/cm; approximately 30 min lapsed before the cells were able to fully follow the direction of the applied field. Possible biophysical bases and pathophysiological significance of the results obtained are discussed.

Keywords Prostate · Cancer · MAT-LyLu cells
AT-2 cells · Fractal dimension

Z. Siwy (✉)
Materials Research Department,
Gesellschaft für Schwerionenforschung,
Planckstrasse 1, 64291 Darmstadt, Germany
E-mail: z.siwy@gsi.de
Tel.: +49-6159-712177
Fax: +49-6159-712179

Z. Siwy
Institute of Physical Chemistry and Technology of Polymers,
Silesian University of Technology,
Strzody 9, 44-100 Gliwice, Poland

M. E. Mycielska · M. B. A. Djamgoz
Department of Biological Sciences,
Neuroscience Solutions to Cancer Research Group,
Imperial College of Science, Technology and Medicine,
Sir Alexander Fleming Building, London , SW7 2AZ, UK

Introduction

Cellular motility generally has been investigated extensively for many years, and its involvement in such biological processes as tissue morphogenesis, regeneration, wound healing and immune responses of animals is commonly recognized (e.g. Nuccitelli 1988; Mohler 1993; Gold et al. 1997; Banyard and Zetter 1999; Bertuzzi and Gandolfi 2000). The issue of cancer cell mobility, in particular, was taken up originally by Virchov (1863). Subsequent studies discovered that the motility of cancer cells can be related to their metastatic potential; on the whole, there was thought to be a positive relationship between the two aspects (Isaacs et al. 1986; Zetter 1990; Mohler 1993). Examination of cell locomotion, therefore, can facilitate the understanding of the metastatic process, and thus ultimately be useful in the diagnosis and treatment of cancer.

Prostatic epithelial cells would normally be subject to an endogeneous, "standing" direct current (dc) electric field (EF) in the form of a trans-cellular potential in the gland (Szatkowski et al. 2000). However, how the dcEF would affect the motility of the cells early in the metastatic cascade (localized invasion) is not known. Interestingly, electrodiagnosis of malignancy has been reported, although its cellular/molecular basis is not clear (Fukuda et al. 1996; Faupel et al. 1997; Cuzick et al. 1998). In an earlier study on rat prostate cancer cells, we showed that only the strongly metastatic MAT-LyLu cells possess a clear ability to orient their movement in an external dcEF ("galvanotaxis"), unlike the weakly metastatic AT-2 cells whose response to an electric field was much weaker and in

the opposite direction (Djamgoz et al. 2001). This finding followed earlier work which showed distinct electrophysiological and galvanotactic responses of strongly and weakly metastatic cells of rat and human prostate carcinoma (Grimes et al. 1995; Laniado et al. 1997; Smith et al. 1998; Foster et al. 1999; Djamgoz et al. 2001). A particularly interesting result was the identification of functional voltage-gated sodium channels (VGSCs), expressed selectively in the strongly metastatic cells (Grimes et al. 1995; Laniado et al. 1997; Grimes and Djamgoz 1998; Fraser et al. 2000). Importantly, pharmacological blockage of VGSC activity in the MAT-LyLu cells suppressed galvanotaxis (Djamgoz et al. 2001), consistent with the occurrence of functional VGSCs specifically in the strongly metastatic phenotype (Grimes et al. 1995; Laniado et al. 1997).

Fractal methods have been found to be useful in studying locomotion. For example, such an approach provided new quantitative measures of sperm motility and could differentiate between hyperactivated or non-hyperactivated states (e.g. Katz and George 1985; Davis and Siemers 1995; Mortimer et al. 1996; Mortimer 1998). Other applications include characterization of the movements of the marine prosobranch, *Littorina littorea*, during mating and non-mating seasons (Erlandsson and Kostylev 1995), and swimming in clownfish (Coughlin et al. 1992). "DNA walks" were also studied by fractal methods, and it was shown that a stronger correlation existed with the coding parts of the genes than the non-coding parts (Abramson et al. 1999). Interestingly, it has also been found that the fractal characteristics of chromatin can be correlated with breast cancer (Einstein et al. 1998).

In our earlier galvanotaxis study on rat prostate cancer cells, some basic motility parameters were determined and compared for two cell lines (MAT-LyLu and AT-2), contrasting in their metastatic potential (Djamgoz et al. 2001). In the present work, we have extended the statistical analysis of cell motility and broadened the quantitative approach to the application of fractal methods (Mandelbrot 1983; Bassingthwaighte et al. 1994; Schuster 1995). In addition, "random walk" analysis (Havlin and Ben-Avraham 1987) enabled the testing of the possible diffusional characteristics of the cells' locomotion. We have also examined the time course of development of the cells' trajectories in an attempt to evaluate the delay, if any, in the cells' motility becoming directional. Finally, the voltage dependence of the various parameters analysed was determined in order to gain an insight to possible involvement of voltage-dependent (e.g. ion channel) mechanisms.

The results have been divided into two parts, reflecting the major problems addressed. First, we present a detailed comparison of the motility characteristics of strongly versus weakly metastatic cells (MAT-LyLu versus AT-2, respectively) on the basis of their behaviour in a dcEF of 3 V/cm. The second part focuses on the influence of electric field intensity on the various parameters describing the motility of the galvanotactic MAT-LyLu cells.

Materials and methods

Experimental techniques and data acquisition

Experiments were performed on two well-characterized rat prostate cancer ("Dunning") cell lines having markedly different metastatic ability: MAT-LyLu and AT-2 cells, which metastasize in $>90\%$ and $<10\%$ of cases, respectively, when injected into Copenhagen rats (Isaacs et al. 1986). The cells were cultured as described previously (Grimes et al. 1995; Djamgoz et al. 2001). Cellular migration and response to the electric field were assayed using a galvanotaxis apparatus described in detail by Korohoda et al. (2000) and Djamgoz et al. (2001). MAT-LyLu and AT-2 cells ($n=50$ each) were tracked for 360 min, using time-lapse images taken at 5 min intervals; an individual cell's trajectories were constructed from 73 successive cell centroid positions (Korohoda and Madeja 1997; Korohoda et al. 1997; Djamgoz et al. 2001). The data were stored in a two-column matrix of x and y coordinates at successive time points (t_i). Comparison of MAT-LyLu and AT-2 cells' motilities were performed at the criterion field strength of 3 V/cm. The dependence of MAT-LyLu cells' motility on the dcEF strength was determined in the range 0.3–3 V/cm.

Parameters measured

The motilities of MAT-LyLu and AT-2 cells in control conditions and in dcEFs were studied by statistical and fractal analyses. The following parameters were determined.

Net displacement

The net displacement (L_n) was defined as the shortest ("direct") distance covered by the cell between the starting point (at time $t=0$) and the final position (at time $t=360$ min). The x and y components of L_n (L_{nx} and L_{ny}) were also calculated. From these, the average speed of movement (V_n) and the velocities in the x and y directions (V_{nx} and V_{ny}) could be obtained. In addition, the relative occurrence of given cells in the cathode and anode halves of the electric field (F_c and F_a) was determined as a percentage of the x and y coordinates being positive and negative, respectively.

Total length of cell trajectory

The total length of the cell trajectory (L_t) was the real distance covered by the cell, calculated as the sum of the unitary jumps performed in successive 5-min intervals, according to the formula:

$$L_t = \sum_{i=1}^{n-1} \sqrt{[x(t_{i+1}) - x(t_i)]^2 + [y(t_{i+1}) - y(t_i)]^2} \quad (1)$$

where n is the total number of the trajectory points ($n=73$), and $x(t_i)$, $y(t_i)$, $x(t_{i+1})$, $y(t_{i+1})$ denote the coordinates of the successive positions of the cell, separated by the 5-min recording interval.

Coefficient of movement efficiency

The coefficient of movement efficiency (CME) was defined as L_n/L_t, representing a normalized measure of the straightness of the trajectories (Djamgoz et al. 2001). The values of CME would be in the range 0–1, corresponding to the displacement being null and straight, respectively.

Instantaneous velocities

The instantaneous velocities (V_{ix} and V_{iy}) in the x and y directions were calculated from the following definitions:

$$V_{ix} = x(t_{i+1}) - x(t_i) \quad (2)$$

$$V_{iy}=y(t_{i+1})-y(t_i) \quad (3)$$

In particular, since the electric field was applied along the x-axis, positive and negative values of V_{ix} would indicate movement directly towards the cathode and the anode, respectively.

Orientation

The orientation (β) of cell movement was defined (in radians) as the net angle β between the straight line joining the cell's given position to the origin and the x-axis, i.e.:

$$\beta = \text{arctg}\frac{y(t_i)}{x(t_i)} \quad (4)$$

The range of β was −3.14 to 3.14 radians.

Dimension of random walk

The dimension of random walk (d_w) described the diffusional character of cell movement and was defined through the power law scaling of the variance σ with time (Gardiner 1990; Havlin and Ben-Avraham 1987). Accordingly:

$$\sigma \propto t^{1/d_w} \quad (5)$$

The variance σ was defined as $\sqrt{[x(t)-x(t_0)]^2+[y(t)-y(t_0)]^2}$ and averaged over the whole population for each cell type. The above relation (Eq. 5) in double-logarithmic coordinates would be a straight line, the slope of which gives the value of d_w. For the dimension of random walk, $d_w=2$ would indicate random movement; $d_w<2$ would indicate directional movement relative to the applied dcEF; and $d_w>2$ would indicate a process slowing down the cells' movement.

Fractal dimension (d_f)

The fractal dimension (d_f) was defined through the notion of a homogeneous function (Liebovitch et al. 1987; Grzywna et al. 1999), as follows:

$$L(at) = a^{d_T-d_f}L(t) \quad (6)$$

where $L(t)$ is the total length of cell trajectory when using the time scale t; a stands for the scaling parameter (e.g. $a=2$ would correspond to the length of a trajectory created by connecting every second point of the recorded data); d_T is a topological dimension ($d_T=1$ for all smooth curves; $d_T=2$ for objects like squares and triangles). The fractal dimension d_f was calculated by linear regression performed on a double-logarithmic plot (Mandelbrot 1983; Liebovitch et al. 1987). Thus, d_f specified the relation between the time series measured with different sampling frequencies. On the basis of previous studies on the minimum length of the cell trajectory needed for the reliable determination of d_f (e.g. Mortimer 1998), a 73-point trajectory was deemed appropriate for the present analysis.

Data analysis

The data were analysed using the software Matlab 5.3 (MathWorks). The distributions and the mean values of all the parameters were calculated, together with the standard deviations. The time course and voltage dependency of the various parameters were also studied. The significance of the results, including comparisons of the two contrasting cell types studied, was determined using Student's t-test. Values of $P<0.05$ were assumed to represent significance.

Results

The quantitative data obtained are summarized in Table 1.

Comparison of the cells' basic motility characteristics

Typical trajectories of MAT-LyLu and AT-2 cells in control conditions and in an applied dcEF of 3 V/cm are illustrated in Fig. 1. Under the control conditions used, the motility characteristics of the MAT-LyLu and AT-2 cells appeared similar (Fig. 1A, C); there was no significant difference as regards the total length of trajectory, net displacement, coefficient of movement efficiency, instantaneous velocities, orientation of cell movement with dcEF direction, or the fractal dimension (Table 1). In contrast, the presence of the dcEF revealed a significant difference between the two cell lines (Fig. 1B vs. D): MAT-LyLu cells responded much more strongly than the AT-2 cells; the former moved briskly towards the cathode, while AT-2 cells showed a tendency of moving towards the anode. Comparison of the total length of the cells' trajectories showed that the non-directional motility was the same for both cell lines (Table 1). Only the net displacement, which is influenced by the directionality of movement, differed between the two cell lines. Application of 3 V/cm dcEF increased L_n of MAT-LyLu cells more than three-fold. The value of L_n for the AT-2 cells remained unaffected by the applied voltage (Table 1).

Studies of the x and y components of L_n enabled the determination of the velocities towards the cathode and the anode, respectively. Application of the 3 V/cm dcEF brought about a significant (more than five-fold) increase in the average velocity towards the cathode, from 0.07 ± 0.05 μm/min in control conditions to 0.37 ± 0.35 μm/min in the field ($P<0.05$). Consistent with this, the relative occurrence of the MAT-LyLu cells in the cathode half of the electric field increased from 41% to 95%. On the other hand, the y-component of L_n and hence V_y were not affected by the applied field.

The instantaneous velocities of MAT-LyLu and AT-2 cells also were the same, under both the control conditions and in the field (Table 1). This implied that the lengths of the cells' unitary jumps were independent of the external conditions. However, the dcEF increased the number of unitary jumps towards the cathode for the MAT-LyLu cells. Thus, the percentage of positive jumps towards the cathode (V_{ix}^+) in the field was more than twice that of negative jumps (V_{ix}^-). In the case of the AT-2 cells, V_{ix}^+ and V_{ix}^- also became unequal in the field, albeit to a lesser extent. The percentage of negative V_{ix}, reflecting the preferential movement towards the anode, was 37%, while the percentage of movement towards the cathode was significantly smaller (31%; $P=0.04$).

The increased directionality of the movement of MAT-LyLu cells in dcEF was confirmed by analyses of the coefficient of movement efficiency and the fractal dimension. Both parameters revealed further the tendency for the straightening of the trajectories by the applied electric field. The procedure of CME determination required averaging over the whole trajectory and, therefore, was not sensitive to any local intricacy. On the other hand, the values of d_f and d_w were strongly influenced by the local pattern of a trajectory, and therefore

Table 1 Summary of quantitative data (means ± standard deviations) obtained from MAT-LyLu and AT-2 cells under control conditions and in the presence of a dcEF of 3 V/cm. All the parameters are defined in Materials and methods. For each parameter, the data were averaged from 50 cells

Parameter	MAT-LyLu		AT-2	
	Control	3 V/cm	Control	3 V/cm
Total length of cell trajectory, L_t (μm)	344 ± 48.5	364 ± 91	320 ± 53.2	353 ± 58.9
Net displacement, L_n (μm)/net speed, V_n (μm/min)	40.6 ± 32.8/ 0.11 ± 0.09	142 ± 125/ 0.39 ± 0.35	38.3 ± 23.5/ 0.11 ± 0.07	46.2 ± 33.1/ 0.13 ± 0.10
Average L_{nx} on the cathode side, $< L_{nx} >_c$ (μm)/ average speed on the cathode side, $(V_{nx})_c$ (μm/min)	23.4 ± 16.5/ 0.07 ± 0.05	134 ± 126/ 0.37 ± 0.35	26.0 ± 18.9/ 0.07 ± 0.05	12.6 ± 9.61/ 0.04 ± 0.03
Average L_{nx} on the anode side, $< L_{nx} >_a$ (μm)/ average speed on the anode side: $(V_{nx})_a$ (μm/min)	−27.2 ± 18.0/ −0.08 ± 0.05	–	−34.4 ± 25.6/ −0.10 ± 0.07	−33.2 ± 25.9/ −0.09 ± 0.07
Average L_{ny} over the positive values (μm)/ average speed towards the cathode, V_{nx}^+ (μm/min)	23.1 ± 16.8/ 0.06 ± 0.05	21.9 ± 21.6/ 0.06 ± 0.06	17.5 ± 15.7/ 0.05 ± 0.04	23.1 ± 19.5/ 0.06 ± 0.05
Average L_{ny} over the negative values (μm)/ average speed towards the anode, V_{nx}^- (μm/min)	−23.0 ± 16.7/ −0.06 ± 0.05	−39.0 ± 34.8/ −0.11 ± 0.10	−20.2 ± 16.6/ −0.06 ± 0.05	−35.6 ± 33.8/ −0.10 ± 0.09
Relative occurrence of given cells in the cathode half of the electric field, F_c (%)	41	95	44	25
Relative occurrence of given cells in the anode half of the electric field, F_a (%)	49	3	48	67
Percentage of the total time (6 h) the given cells stay in the starting point of the trajectory, $x = 0$ (%)	10	2	8	8
Percentage of the total time (6 h) the given cells stay in the positive half of the coordinate system, $y > 0$ (%)	57	40	43	39
Percentage of the total time (6 h) the given cells stay in the negative half of the coordinate system, $y < 0$ (%)	34	52	46	53
Percentage of the total time (6 h) the given cells stay in the starting point of the trajectory, $y = 0$ (%)	9	8	11	8
Instantaneous velocity of movement towards the cathode, V_{ix}^+ (μm/min)	0.87 ± 0.48	1.02 ± 0.59	0.82 ± 0.42	0.82 ± 0.41
Instantaneous velocity of movement towards the anode, V_{ix}^- (μm/min)	−0.90 ± 0.49	−0.77 ± 0.39	−0.82 ± 0.39	−0.86 ± 0.46
Coefficient of movement efficiency, CME	0.12 ± 0.08	0.35 ± 0.22	0.12 ± 0.07	0.13 ± 0.09
Orientation, β (radian)	0.52 ± 1.8	−0.04 ± 0.71	−0.51 ± 0.04	−0.13 ± 2.16
Dimension of random walk, d_w	1.8 ± 0.2	1.1 ± 0.1	1.9 ± 0.2	1.6 ± 0.2
Fractal dimension, d_f	1.7 ± 0.2	1.5 ± 0.2	1.7 ± 0.2	1.6 ± 0.2

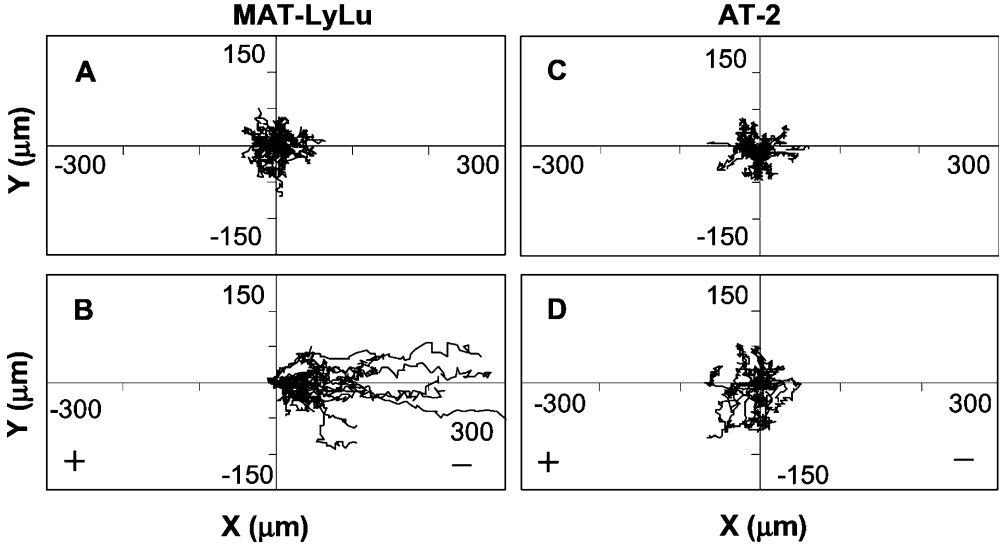

Fig. 1 Typical examples of trajectories of MAT-LyLu and AT-2 cells under control experimental conditions (**A**, **C**) and in a direct-current electric field of intensity 3 V/cm (**B**, **D**). Each panel is the composite of 25 cells. The starting point for all the cells was fixed as the origin (0, 0). The electric field was applied along the *x*-axis (indicted by +/−)

would be more sensitive in distinguishing changes of the cells' motility by dcEF. The fractal dimension decreased significantly for both cell lines ($P = 0.01$ for each cell), which suggested that the slight response of the AT-2 cells to the field was also significant. This conclusion was supported independently by the random walk analyses, which also showed that the movement of the MAT-LyLu cells in the electric field could not be treated as random walk but rather represented a directional migration under the influence of the applied dcEF (d_w falling from 1.8 to 1.1); the same, but with a smaller effect, was observed for the AT-2 cells (d_w falling from 1.9 to 1.6).

In order to obtain information about orientation of movement, average values as well as the distributions of the angle β were determined (Fig. 2; Table 1). Under the control conditions, both cell types moved in all directions with equal probability (Fig. 2A, C). On the other hand, the unimodal character of the histogram found for the MAT-LyLu cells in dcEF (Fig. 2B) confirmed the strong directional responses of the cells to the applied field. The increase of the frequency of occurrence of large negative and positive values of β for the AT-2 cells (Fig. 2D) indicated their slight preferential movement in the opposite direction.

Heterogeneity of MAT-LyLu cells

In order to gain an insight into possible heterogeneity in the MAT-LyLu cell population studied, the distribution of each parameter was determined in individual histograms. As an example, Fig. 3 presents the histograms of CME values for MAT-LyLu and AT-2 cells. Under the control condition, both cell lines had similar distributions, peaking at around 0.2 (clear bars; Fig. 3A, B). In the presence of the field, however, there was a significant shift towards 1 and broadening of the distribution of CME values for the MAT-LyLu cells (dark bars; Fig. 3A). No such obvious change was seen for the AT-2 cells (dark bars; Fig. 3B). It thus appeared that the directionality of the response of the strongly metastatic cell line in the applied dcEF had much greater heterogeneity overall.

Time dependency of the MAT-LyLu cell motility parameters

In order to examine the time course of development of trajectories of MAT-LyLu cells, the net displacement L_n, the instantaneous velocity V_{ix}, and the angle β were studied as a function of time. Figure 4A–C shows the typical time dependence of the three parameters under control conditions. These data suggested that all the parameters changed randomly in time, without revealing any regular pattern. Figure 4D–F presents an example of the time dependence of L_n, V_{ix} and β for a MAT-LyLu

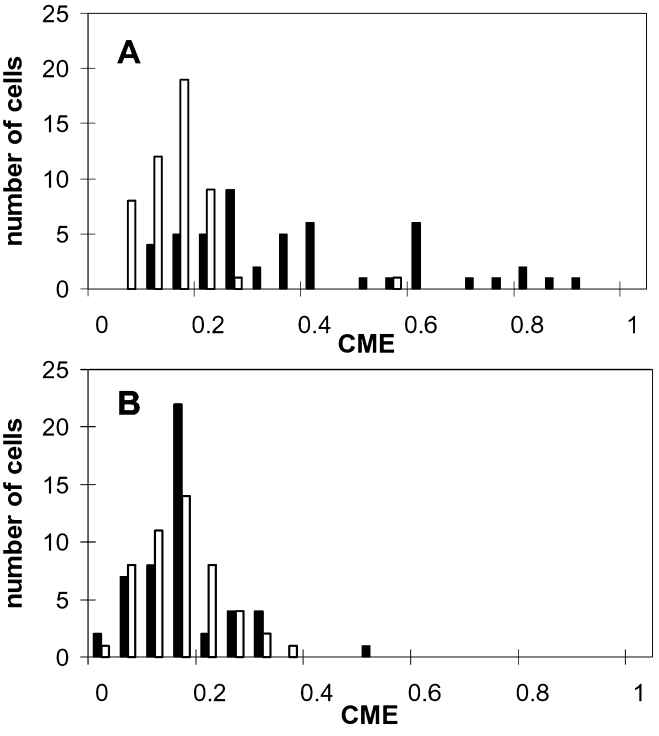

Fig. 3 Histograms showing the distributions of the values of the coefficient of movement efficiency (CME) for MAT-LyLu (**A**) and AT-2 cells (**B**) recorded under control conditions (*light bars*) and in an electric field of 3 V/cm (*dark bars*)

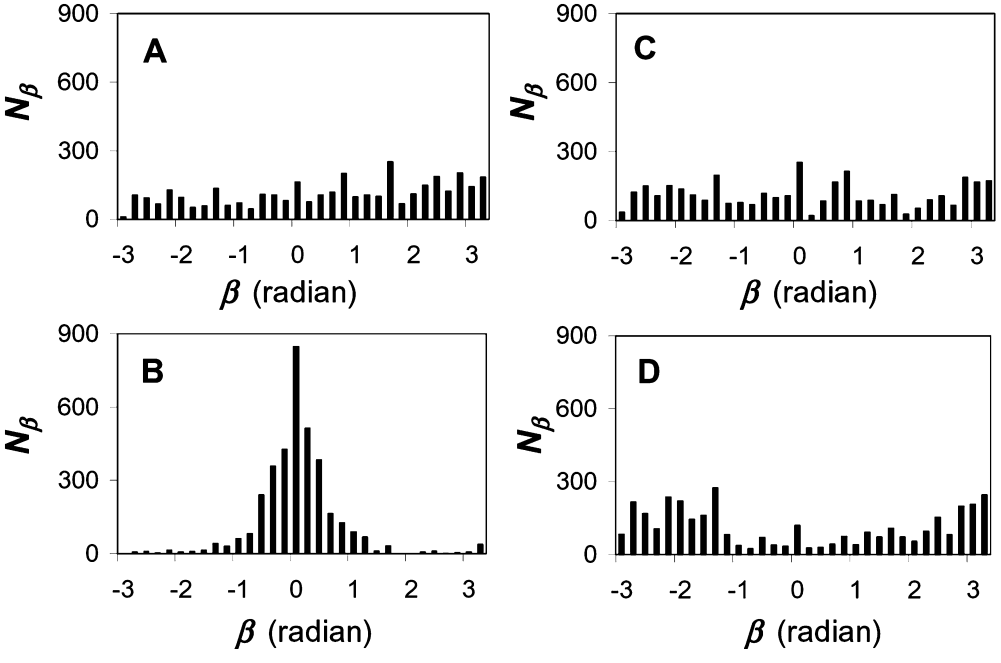

Fig. 2 Histograms showing the distributions of the values of angle β for MAT-LyLu cells under control conditions (**A**) and in an electric field of 3 V/cm (**B**). **C**, **D** denote comparable data for the AT-2 cells in control conditions and in an electric field (also 3 V/cm), respectively. The angle β was as defined by Eq. (4) in Materials and methods. N_β is the number of values of β in given "bins" of the histograms

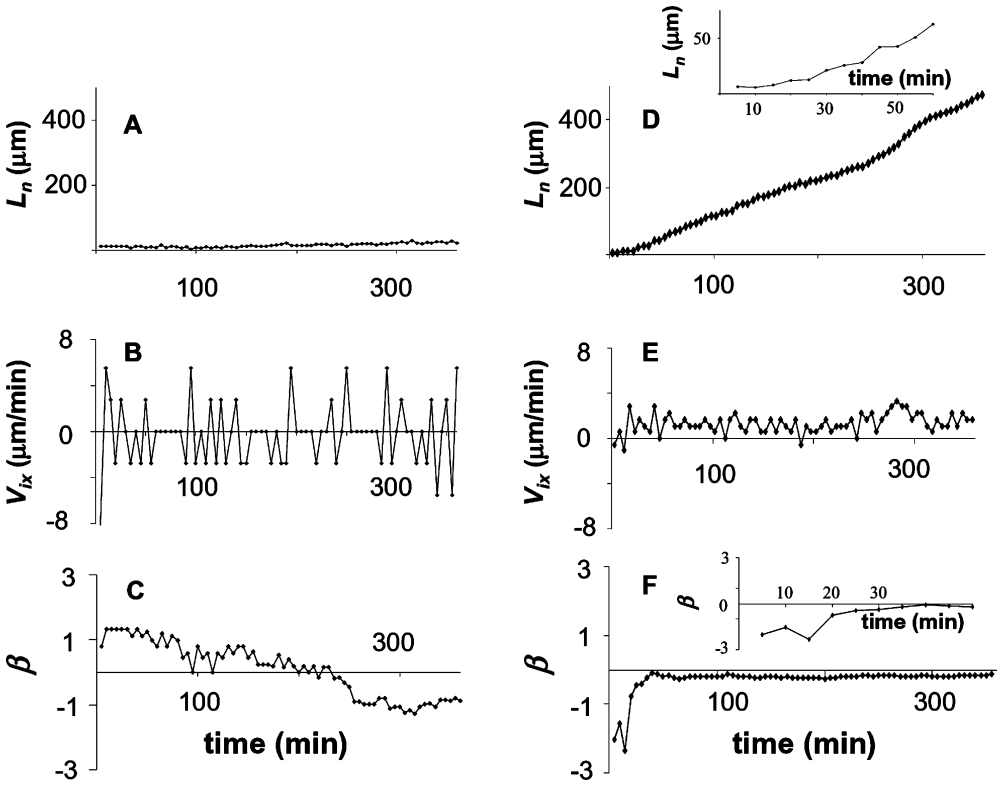

Fig. 4 Examples of the time dependence of the parameters L_n (**A**, **D**), V_{ix} (**B**, **E**) and β (**C**, **F**) for typical MAT-LyLu cells (CME > 0.5). **A**–**C**: data obtained under control conditions. **D**–**F**: data obtained from a cell exposed to a dcEF of 3 V/cm. *Insets* in **D** and **F** show on expanded scales the time dependence of L_n and β, respectively

cell in a dcEF of 3 V/cm (CME > 0.5). "Smoothing" of β and stabilization of the sign of V_{ix} were complete within approximately 30 min after applying the field. Moreover, the modified values were maintained for the rest of the recording period (6 h) without any further change, i.e. there was no adaptation to the applied, sustained field; 30 min were also needed for the onset of linear increase of L_n in time.

This analysis was repeated at dcEFs of 0.6 and 0.9 V/cm. In those cases, no real smoothing of the time dependence of β occurred; only after approximately 50 min did the values diminish, but remained fluctuating between 0.6 and +0.6 radians (not illustrated). It was concluded that response to the applied dcEF was generally faster when the field was made stronger.

Dependence of the galvanotactic response parameters of MAT-LyLu cells on dcEF strength

Typical trajectories of MAT-LyLu cells in dcEFs in the range 0–3 V/cm are shown in Fig. 5. On the whole, a higher voltage brought about a more pronounced movement towards the cathode. This is seen clearly for the orientation of movement, illustrated by the histograms of the angle β (Fig. 6). Thus, as the dcEF strength increased, the probability of movement towards the cathode increased (β tending towards 0).

Figure 7A–E presents in more detail the dependence of L_t, CME, L_n, d_w and d_f parameters on the applied voltage. These data are presented as relative percent change with respect to the original value treated as 100%. The value of L_t was not affected by the strength of the applied dcEF, the only parameter to show this behaviour (Fig. 7A). Thus, the total length of trajectory covered by a cell (i.e. speed of movement) was independent of the field strength. Figure 7B shows that a significant change (increase) in CME occurred when the field strength reached 0.6 V/cm. Interestingly, continuing to increase the dcEF strength up to 3 V/cm had no further effect on the value of CME, i.e. the effect was all-or-none. A significant increase in L_n also occurred when the value of dcEF reached 0.6 V/cm (Fig. 7C). As the field was made stronger, there was no further change up to 1.5 V/cm. However, a significant increase was seen at 3 V/cm, the strongest dcEF tested ($P < 0.05$). In the random walk analysis (Fig. 7D), for 0 and 0.3 V/cm, the cells performed random walk ($d_w = 2.0 \pm 0.3$). The value of d_w became significantly smaller than 2 ($d_w = 1.5 \pm 0.1$) for 0.6 V/cm. As the field strength was increased, the value of d_w decreased further, and the cells performed fully directional movement at 3 V/cm, suggested by the value of d_w close to unity. Analysis of the fractal dimension d_f also revealed a mixed dependence on dcEF strength (Fig. 7E). There was no effect at 0.3 V/cm. A significant decrease in the value of d_f was seen at 0.6 V/cm, and this was maintained, remaining saturated up to 3 V/cm, except at 1.5 V/cm where a significant decrease was seen (Fig. 7E).

From these analyses, therefore, two generalities emerged as regards the voltage dependency of the cell motility parameters studied, as follows:

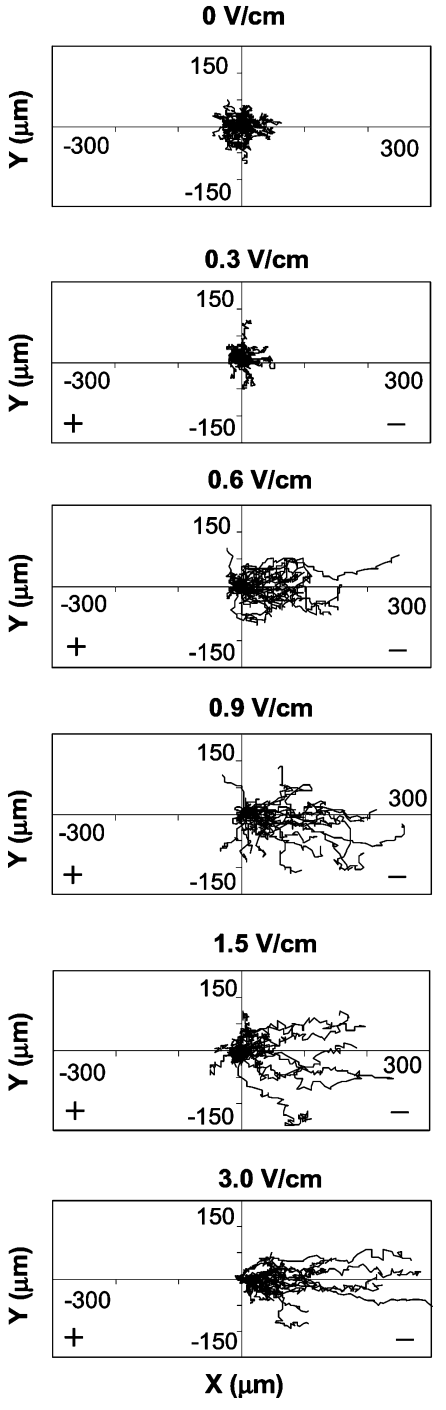

Fig. 5 Typical trajectories of MAT-LyLu cells exposed to dcEFs of different intensities in the range 0–3 V/cm (values indicated above each panel). Each set represents the composite of 25 cells' trajectories, plotted as in Fig. 1

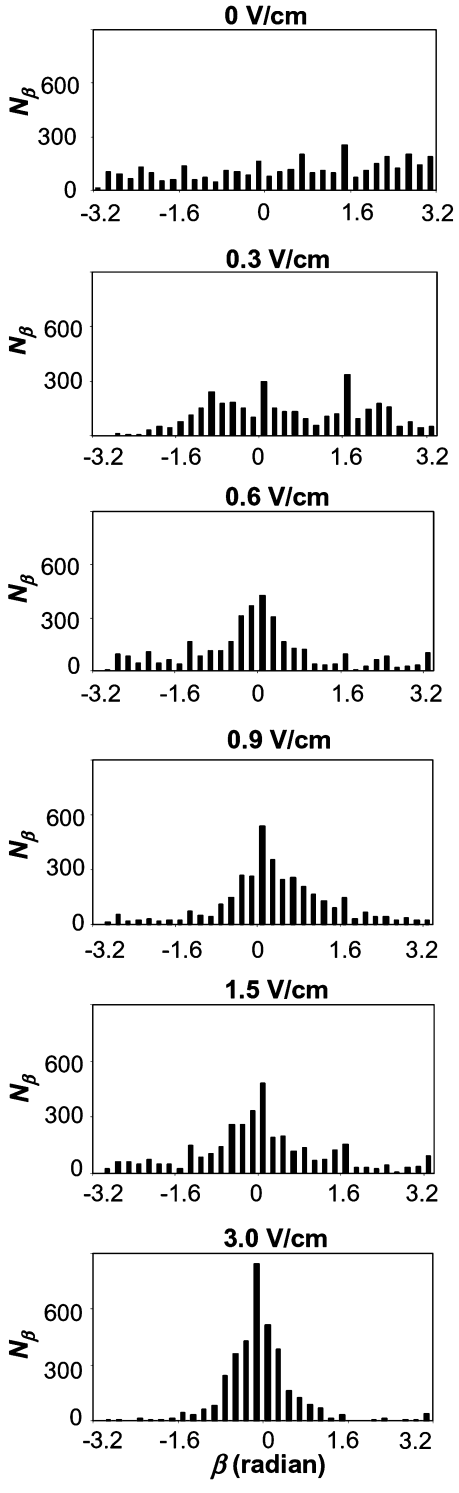

Fig. 6 Histograms of values of the angle β for MAT-LyLu cells exposed to dcEFs of different intensities in the range 0–3 V/cm (values indicated above each panel). Each data set was obtained from 50 representative cells. The angle β was defined by Eq. (4). N_β is the number of values of β in given "bins" of the histograms

1. All the parameters, except one, were associated with a dcEF "threshold" of 0.6 V/cm. The exception was L_t, which was not affected at all by the applied voltage.
2. All the parameters (CME, L_n, d_w and d_f) that responded to the dcEF had an "all-or-none" type characteristic, at least for a part of the voltage range tested, and some indication of multiple voltage domains.

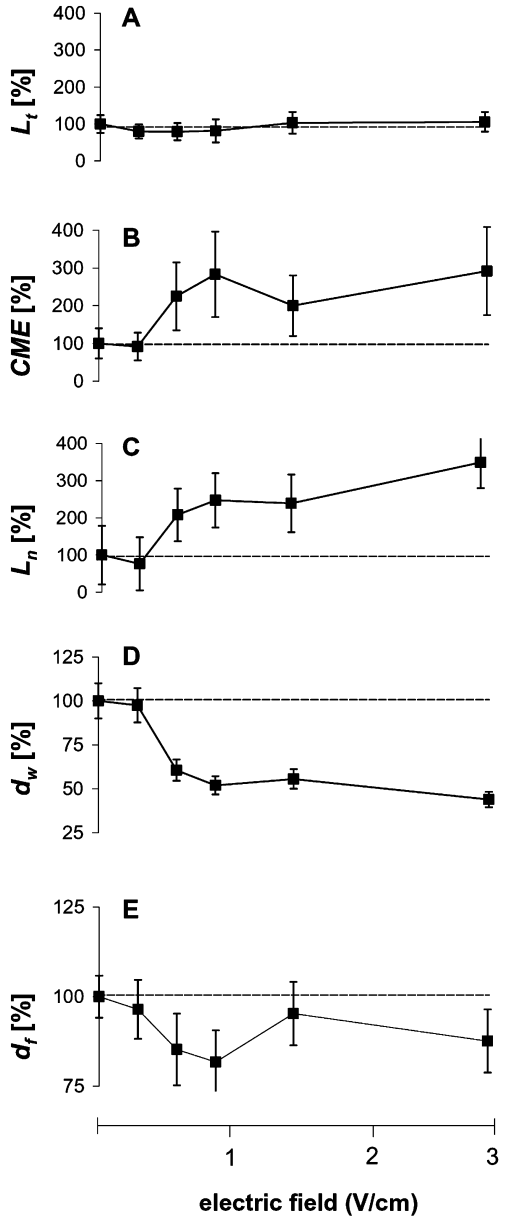

Fig. 7 Dependence of the parameters L_t (**A**), CME (**B**), L_n (**C**), d_w (**D**) and d_f (**E**) determined for MAT-LyLu cells exposed to electric field intensities in the range 0–3 V/cm. The field was applied at $t=0$. For each parameter, data were averaged from 50 cells, and are presented as percentages of the respective original values (means ± standard deviations)

Discussion

The galvanotactic responses of strongly and weakly metastatic rat prostate cancer cells (MAT-LyLu and AT-2, respectively) were studied for the first time by detailed statistical and fractal analyses. The main problems addressed were: (1) possible differences in the galvanotactic properties of the two cell lines, as characterized by the different motility parameters; (2) dependence of the highly metastatic cells' response to the electric field of different intensity; (3) diffusional characteristics of the locomotion of MAT-LyLu and AT-2 cells; and (4) the time dependency of the cells' response to the applied dcEF.

Basic effects of electric field on MAT-LyLu and AT-2 cells' motility

Visual observation of the trajectories of MAT-LyLu and AT-2 cells in dcEF immediately revealed directional movement towards the cathode for the strongly metastatic cell line, whilst the weakly metastatic cells tended to move towards the anode (Fig. 1). The various parameters integral to this phenomenon (''galvanotaxis'') were analysed by application of several different quantitative measures (Table 1). In particular, introduction of the independent fractal parameter d_f and the dimension of random walk d_w complemented and extended the original statistical analysis (Djamgoz et al. 2001). The fractal analysis confirmed many of the general characteristics emerging from the examination of the other motility parameters and revealed in addition that dcEFs have a significant effect also on the AT-2 cells (Table 1). The fractal analysis would take into account the local ''structure'' of the cells' trajectories and can ''detect'' geometrical features, unlike, for example, the ''comparable'' CME which is an average measure not ''sensitive'' enough to reveal the multiple voltage domains. The dimension of random walk enabled us to follow any change in the motility characteristics of the MAT-LyLu cells as the dcEF strength was increased. This showed that the cells' movement was completely ''diffusional'' at low or no dcEF, whilst a dcEF of 3 V/cm brought about fully directional movement ($d_w \approx 1$). The parameter d_w, therefore, has a clear physical meaning showing the influence of the external force, originating from the applied dcEF, on the cells' locomotion, and also complements the statistical analyses.

Directionality of the cell movement in the applied dcEFs was also studied by the distribution of the net angle of orientation β (Fig. 2). The β histogram had a peak at $\beta=0$, consistent with directional movement of the MAT-LyLu cells towards the cathode. In contrast, the AT-2 cells moved slightly towards the anode, indicated by the modest shift towards the large negative and positive β angles. The significance of the galvanotactic response of the AT-2 cells was confirmed by the analyses of F_c and F_a (Table 1). This is the first quantitative study of the galvanotactic response of the weakly metastatic AT-2 cells, which would be worthwhile extending.

Time dependency of MAT-LyLu cells' response to dcEF

The time dependence of the parameters V_{ix}, β and L_n was analysed here for the first time (Fig. 4). This revealed that a time delay of some 30 min was necessary for the MAT-LyLu cells to respond do a dcEF (3 V/cm)

by full directional movement. Interestingly, the shortest time after which a cell gave just a detectable response to an applied dcEF was reported earlier to be less than 1 min (Djamgoz et al. 2001). This would imply that MAT-LyLu cells' galvanotactic response may have two levels of time dependence (M.E. Mycielska and M.B.A. Djamgoz, in preparation). The first reaction is very fast and may involve a change such as redistribution of surface charge (Abercrombie and Ambrose 1962; Price et al. 1987; Carter and Coffey 1988; Carter et al. 1989), and subsequent change in membrane potential and voltage-gated ion channel activity (Djamgoz et al. 2001). The second, slower phase could represent cytoskeletal changes, and possibly protein electrophoresis. Preliminary immunocytochemical observations of MAT-LyLu cells excluded the existence of any asymmetry in the distribution of VGSC protein over the cell surface under control conditions (unpublished results). The situation in dcEF is not known, however, and some proteins have been shown to be redistributed in dcEF (Poo and Robinson 1977; Orida and Poo 1978; Stollberg and Fraser 1988). The 30-min time delay of the onset of directional movement could indicate the possibility of some gross redistribution of VGSCs (or other) protein in the membrane by electrophoresis. Once established, however, the motility characteristics were maintained for the length of the cell recordings (6 h), suggesting that the changes induced by the dcEF were long lasting and were such as to put the cells into a new steady state. We have shown previously that voltage-gated Na^+ channel (VGSC) activity has a significant involvement in the MAT-LyLu cells' galvanotactic response (Djamgoz et al. 2001).

Voltage dependency of MAT-LyLu cells' motility parameters

The different analyses applied to the MAT-LyLu cells gave a consistent result, suggesting, firstly, that the effect of the dcEF on the cells' trajectories was non-linear (Figs. 5 and 7). L_t was the only parameter not influenced by the dcEF (Fig. 7A). This is in agreement with the previous result showing that an electric field brings about mainly directionality, rather than speed, of the cell movement. The rest of the parameters studied revealed consistently: (1) a threshold dcEF of 0.6 V/cm; and (2) a tendency to saturate at 1 or 1.5 V/cm, indicating at least a partial "all-or-none" type dependence (Fig. 7B–E). Both aspects (threshold dcEF and apparent all-or-none behaviour) are basic characteristics of VGSC activity which (a) was found specifically in strongly metastatic cells (Grimes et al. 1995); and (b) was shown previously to be involved in the cells' galvanotactic response (Djamgoz et al. 2001). In addition, the observed heterogeneity (Fig. 3) is consistent with only a sub-population of MAT-LyLu cells expressing functional VGSCs (Grimes et al. 1995). On the other hand, a further domain (1.5–3 V/cm) was seen in the voltage dependence of the parameters affected. This would imply that there could be other mechanisms, additional to VGSC, also involved in the cells' galvanotaxis. This agrees with our earlier result showing that blocking VGSC activity with tetrodotoxin did not completely block galvanotaxis. Further work is required to elucidate the range and sequential action of the biophysical mechanisms responsible for the full galvanotactic response of the MAT-LyLu cells.

The phenomenon of galvanotaxis is likely to occur in vivo due to the presence of trans-epithelial potentials in the prostate gland and could be involved in local invasion of tissue early in the onset of prostate cancer (Szatkowski et al. 2000). In overall conclusion, therefore, we would like to suggest that further studies of this phenomenon and analytical description of its biophysical basis may, in the long term, facilitate identification and development of novel targets for treating metastatic disease.

Acknowledgements We are grateful to The British Council (Warsaw) and NATO (Scientific Division) for financial support in the form of travel/twinning grants.

References

Abercrombie M, Ambrose EJ (1962) The surface properties of cancer cells: a review. Cancer Res 22:25–548

Abramson G, Cerdeira HA, Bruschi C (1999) Fractal properties of DNA walks. Biosystems 49:63–70

Banyard J, Zetter BR (1999) The role of cell motility in prostate cancer. Cancer Metastasis Rev 17:449–458

Bassingthwaighte JB, Liebovitch LS, West BJ (1994) Fractal physiology. Oxford University Press, Oxford

Bertuzzi A, Gandolfi A (2000) Cell kinetics in a tumour cord. J Theor Biol 204:587–599

Carter HB, Coffey DS (1988) Cell surface charge in predicting metastatic potential of aspirated cells from the Dunning rat prostatic adenocarcinoma model. J Urol 140:173–175

Carter HB, Partin AW, Coffey DS (1989) Prediction of metastatic potential in an animal model of prostate cancer: flow cytometric quantification of cell surface charge. J Urol 142:1338–1341

Coughlin DJ, Strickler JR, Sanderson B (1992) Swimming and search behaviour in clownfish, *Amphion perideraion*, larvae. Anim Behav 44:427–440

Cuzick J, Holland R, Barth V, Davies R, Faupel M, Fentiman I, Frischbier HJ, LaMarque JL, Merson M, Sacchini V, Vanel D, Veronesi U (1998) Electropotential measurements as a new diagnostic modality for breast cancer. Lancet 352:359–363

Davis RO, Siemers RJ (1995) Derivation and reliability of kinematic measures of sperm motion. Reprod Fertil Dev 7:857–869

Djamgoz MBA, Mycielska M, Madeja Z, Fraser SP, Korohoda W (2001) Directional movement of rat prostate cancer cells in direct-current electric field: control by voltage-gated Na^+ channel activity. J Cell Sci 114:2697–2705

Einstein AJ, Wu Hai-Shan, Gil J (1998) Self-affinity and lacunarity of chromatin texture in benign and malignant breast epithelial cell nuclei. Phys Rev Lett 80:397–400

Erlandsson J, Kostylev V (1995) Trail following, speed and fractal dimension of movement in a marine prosobranch, *Littorina littorea*, during a mating and a nonmating season. Marine Biol 122:87–94

Faupel M, Vanel D, Barth V, Davies R, Fentiman IS, Holland R, Lamarque JL, Sacchini V, Schreer I (1997) Electropotential evaluation as a new technique for diagnosing breast lesions. Eur J Radiol 24:33–38

Foster CS, Cornford P, Forsyth L, Djamgoz MBA, Ke Y (1999) The cellular and molecular basis of prostate cancer. Br J Urol 83:171–194

Fraser SP, Grimes JA, Djamgoz MBA (2000) Effects on voltage-gated ion channel modulators on rat prostatic cancer cell proliferation: comparison of strongly and weakly metastatic cell lines. Prostate 44:61–76

Fukuda M, Shimizu K, Okamoto N, Arimura T, Ohta T, Yamaguchi S, Faupel ML (1996) Perspective evaluation of skin surface electropotentials in Japanese patients with suspicious breast lesions. Jpn J Cancer Res 87:1092–1096

Gardiner W (1990) Handbook of stochastic methods. Springer, Berlin Heidelberg New York

Gold JS, Bao L, Ghoussoub RA, Zetter BR, Rimm DL (1997) Localization and quantitation of expression of the cell motility-related protein thymosin beta15 in human breast tissue. Mod Pathol 10:1106–1112

Grimes JA, Djamgoz MBA (1998) Electrophysiological characterization of voltage-activated Na^+ current expressed in highly metastatic MAT-LyLu cell line of rat prostate cancer. J Cell Physiol 369:290–294

Grimes JA, Fraser SP, Stephens GJ, Downing JE, Laniado ME, Foster CS, Abel PD, Djamgoz MBA (1995) Differential expression of voltage-activated Na^+ currents in two prostatic tumor cell lines: contribution to invasiveness *in vitro*. FEBS Lett 369:290–294

Grzywna ZJ, Liebovitch LS, Siwy Z (1997) On the self-similarity of the logistic map. Cell Mol Biol Lett 2:4–20

Havlin S, Ben-Avraham D (1987) Diffusion in disordered media. Adv Phys 36:695–798

Isaacs JT, Issacs WB, Feitz WF, Scheres J (1986) Establishment and characterization of seven Dunning rat prostatic cancer cell lines and their use in developing methods for predicting metastatic abilitis of prostatic cancers. Prostate 9:261–281

Katz MJ, George EB (1985) Fractals and the analysis of growth paths. Bull Math Biol 47:273–286

Korohoda W, Madeja Z (1997) Contact of sarcoma cells with aligned fibroblasts accelerates their displacement: computer assisted analysis of tumour cell locomotion in co-culture. Biochem Cell Biol 75:263–276

Korohoda W, Golda J, Sroka J, Wojnarowicz A, Jochym P, Madeja Z (1997) Chemotaxis of *Amoeba proteus* in the developing pH gradient within a pocket-like chamber studied with the computer assisted method. Cell Motil Cytoskel 38:38–53

Korohoda W, Mycielska M, Janda E, Madeja Z (2000) Immediate and long-term galvanotactic responses of Amoeba proteus to dc electric field. Cell Motil Cytoskel 45:10–26

Laniado ME, Lalani EN, Fraser SP, Grimes JA, Bhangal G, Djamgoz MBA, Abel PD (1997) Expression and functional analysis of voltage-activated Na^+ channels in human prostate cancer cell lines and their contribution to invasion *in vitro*. Am J Pathol 150:1213–1221

Liebovitch LS, Fischborg J, Koniarek JP (1987) Ion channel kinetics: a model based on fractal scaling rather than multistate Markov processes. Math Biosci 84:37–68

Mandelbrot BB (1983) The fractal geometry of nature. Freeman, New York

Mohler JL (1993) Cellular motility and prostatic carcinoma metastates. Cancer Metastatis Rev 12:53–67

Mortimer ST (1998) Minimum sperm trajectory length for reliable determination of the fractal dimension. Reprod Fertil Dev 10:465–469

Mortimer ST, Swan MA, Mortimer D (1996) Fractal analysis of capacitating human spematozoa. Hum Reprod 11:1049–1054

Nuccitelli R (1988) Physiological electric fields can influence cell motility, growth, and polarity. Adv Cell Biol 2:213–233

Orida N, Poo MM (1978) Electrophoretic movement and localisation of acetylcholine receptors in the embryonic muscle cell membrane. Nature 275:3–35

Poo M-M, Robinson KR (1977) Electrophoresis of concanavalin A receptors along embryonic muscle cell membrane. Nature 265: 602–605

Price JA, Pethig R, Lai CN, Becker FF, Gascoyne PR, Szent-Gyorgyi A (1987) Changes in cell surface charge and transmembrane potential accompanying neoplastic transformation of rat kidney cells. Biochim Biophys Acta 9:129–136

Schuster HG (1995) Deterministic chaos, 3rd edn. VCH, Weinheim

Smith P, Rhodes P, Shortland AP, Fraser SP, Djamgoz MBA, Ke Y, Foster CS (1998) Sodium channel protein expression enhances the invasiveness of rat and human prostate cancer cells. FEBS Lett 423:19–24

Stollberg J, Fraser SE (1988). Acetylcholine receptors and concavalin A-binding sites on cultured Xenopus muscle cells: electrophoresis, diffusion, and aggregation. J Cell Biol 107:1397–1408

Szatkowski M, Mycielska M, Knowles R, Kho AL, Djamgoz MBA (2000) Electrophysiological recordings from the rat prostate gland in vitro: identified single-cell and transepithelial (lumen) potentials. Br J Urol Int 86:1068–1075

Virchov R (1863) Ueber bewegliche thierische Zellen. Arch Pathol Anat Physiol Klin Med 28: 237–240

Zetter BR (1990) Cell motility in angiogenesis and tumor metastasis. Cancer Invest 8:669–671